

Vibration Analysis of a Turbine Blade under the interaction of air flow

Santosh Rao¹, Subhrata Nagpal²

Department of Mechanical Engineering,
Bhilai Institute of Technology, Durg CG India

ABSTRACT

This paper aims to investigate the vibration characteristics (natural frequencies and mode shapes) and stresses and deformations of a wind turbine blade under steady-state load conditions. With an upwind horizontal axis and three blades measuring 34.125 meters in length and 70 meters in rotor diameter, the WindPACT 1.5MW wind turbine blade was chosen. SOLIDWORKS software was used to create the wind turbine blade model, which was then exported to ANSYS Workbench. The wind blade has been numerically simulated using finite element analysis. The stationary behaviour of the selected wind power blade was deeply examined in the nominal power (max speed of rotation 21.1 rpm). In this research article, three different composite materials have been selected for different parts of the blade to focus on the effect of the type of material on the stress, deformations, and frequencies of wind turbines.

The results have shown the stress, the total deformations and the first eight frequencies of a wind blade of 1.5 MW. It was determined stresses, total deformations, natural frequency and mode shapes of the wind turbine blade. It can be noticed that the distribution of deformation and stress are similar when using three materials (The maximum deformation occurred at the tip region of the blade because it is free to move and the maximum stress occurred in the root region) But the values of stresses and deformation vary with materials. It is evident that stresses and deformations exhibit variation across different materials; the lowest distortion and highest stress values were observed in the case of carbon fibre utilization

Keywords: stress analysis; steady-state load condition; vibration analysis; wind turbine blade.

1.Introduction

The dynamic interplay between a fluid and a solid material takes place in a confined environment, where the solid component is susceptible to undergoing distortions as a result of, or while being exposed to, the movement of the fluid. As a result, these distortions play a defining role in shaping the boundary conditions and overall layout of the fluidic system. Conversely, the scenario able too unfold manner where structure alters flow properties of the fluid, leading to what is termed as fluid-structure interaction problems. These interactions, which encompass the dynamics between fluids and solid, may appear in the form of either a stable state or oscillatory behavior. In cases of oscillatory interactions, the stress experienced by the solid structure prompts movement, with the structure reverting to its original state only after the process repeats itself. The phenomenon of Fluid-Structure Interaction (FSI) can be observed in various contexts such as in the deformation and stresses experienced by materials in a flight aircraft , a rotating wind turbine, or a fast-moving automobiles. FSI can be observed at various natural occurrences and method, playing a crucial role in the analysis of system designs.

The initiation of the blade occurs at the circular hub segment, leading to the transition to the S818 airfoil, followed by the S825 airfoil, and ultimately evolving into the S826 airfoil at the blade tip. All

10.48047/jocaaa.2024.33.07.39

aspects of the blade's geometry, encompassing twist, span, and chord length, were established through the utilization of the WT_Perf analysis [1-2]. We will create a graphical depiction of the tangential speed at the blade tip and compare it to analytical results. The primary aim of the research is to ascertain the efficacy and power output of wind turbines [3].

Owing to its remarkable precision and flexibility, Computational Fluid Dynamics (CFD) garners significant interest among scholars and design practitioners. By virtue of its multifaceted capabilities, CFD not only furnishes dependable aerodynamic coefficient results but also furnishes intricate insights into flow patterns and wake formation [4–7].

Few studies have explored the aeroelastic impact through the utilization of a nonlinear beam model [8]. When designing a wind turbine blade, the consideration of both twist angle and pitch angle is deemed crucial. Particularly, the pitch angle holds significance in determining the efficiency of the wind turbine [9–11]. A limited number of researchers have integrated tip plates into their study to enhance the performance of wind turbine blades by optimizing the pitch angle for maximum power output corresponding to the prevailing wind speed [12]. The adjustment of rotor velocity and angle of blade pitch in heavy wind velocity has also been a focal point for some researchers. They have introduced a robust sliding mode methodology, utilizing blade pitch as a control input to maintain rotor speed at a specified value in the face of uncertainties inherent in the wind turbine model [13]. Given the necessity for proper monitoring of the blade pitch system, a few proposed mechanisms aim to reduce wear on the wind turbine pitch drive [14]. Moreover, owing to the nonlinear nature of wind turbine dynamics and associated uncertainties, researchers have devised diverse pitch control frameworks to enable concurrent enhancement of power regulation and load alleviation via blade pitch control [15,16]. Various approaches akin to multi-criteria logic, including fuzzy logic, and optimization techniques such as genetic algorithms, have been deployed to manage the pitch angle, accommodating nonlinearities and enhancing system stability by mitigating loading effects on wind turbine blades [17,18].

In comparison to the Boundary Element Method (BEM) model, the Computational Fluid Dynamics (CFD) model exhibits higher computational costs; however, it demonstrates the ability to accurately simulate intricate three-dimensional flow patterns and depict realistic fluid dynamics more precisely [19-21]. Variants of low-order aerodynamic models (e.g. BEM model) are employed to characterize aerodynamic loading [22, 23]. Nevertheless, for achieving accurate representation of intricate 3D flow patterns, more sophisticated resolution techniques become necessary. Elaborate descriptions of the blade's composite layups are provided. The aerodynamic forces are assessed through Computational Fluid Dynamics (CFD) while the structural reactions of the blade are ascertained via Finite Element Analysis (FEA). The approach to coupling is grounded on a one-way coupling methodology, wherein aerodynamic forces computed from computational fluid dynamics simulations are transferred to Finite element analysis simulations as loading boundary conditions [24].

The aeroelastic phenomenon arises from the interaction between fluid and structure, known as fluid-structure interaction (FSI), rendering it a critical subject of investigation for design engineers and researchers. Hence, a meticulous FSI modeling approach is imperative to adhere to the standards necessary for the advancement of wind turbine technology [25]. FSI simulations find application in various fields, including aeronautics and turbomachinery [26], by incorporating partitioned coupling mechanisms that can be unidirectional (one-way) or bidirectional (two-way). The bidirectional coupling is further categorized as weakly or strongly connected, with detailed distinctions elucidated in [27]. The adaptable nature of the established FSI model allows its extension to analogous domains

10.48047/jocaaa.2024.33.07.39

like horizontal axis wind turbines [28-30]. The aerodynamic aspect of FSI modeling primarily relies on the Blade Element Momentum (BEM) model [31] due to its efficiency and reasonable level of accuracy. Conversely, in the structural domain of FSI modeling, beam models and Finite Element Analysis (FEA) models emerge as the predominant methods cited in literature [32, 33]. The FEA model is advantageous for its high-fidelity nature, enabling the examination of intricate stress distributions within each layer of a composite blade structure [34] this study, the FEA model has been chosen as the structural element for FSI simulation. Previous research efforts have focused on integrating more advanced techniques, such as Finite element analysis and computational fluid dynamics, into Fluid Structure interaction simulations. A detailed examination of aeroelastic modeling of wind turbine blades can be located in [35]. MacPhee and Beyene [36] formulated a 2D FSI model to replicate the aeroelastic behavior of a symmetric NACA 0012 blade under varying loads. Similarly, Krawczyk et al. [37] established a corresponding 2D FSI model utilizing CFD and FEA for aeroelastic assessment of a NACA 4412 blade. Bagheri and Nejat [38] introduced a 3D FSI model for aeroelastic evaluation of the NREL Phase VI rotor. The 3D FSI model was utilized to examine the pressure coefficient and torque at various blade segments across wind speeds ranging from 7 to 15 m/sec . Through the use of computational fluid dynamics methods, the aerodynamic efficiency of the horizontal axis wind turbine is investigated. The derived CFD findings are contrasted with the GE1500 xle turbine's experimental data and mathematical computation [39]

2. Design of Wind Turbine Model

Wind turbine blade design is accomplished through the consideration of geometric parameters and technical specifications outlined in references [1] and [2]. The wind turbine in question is a traditional upwind horizontal-axis system with three blades, utilizing control mechanisms that are variable in both speed and pitch angle. Detailed information regarding the WindPACT 1.5MW wind turbine can be located in reference [24], with a comprehensive summary of its primary parameters provided in Table 1. The blades consist of three distinct types of aerofoils - thicker aerofoils S818 for the root section, medium thickness aerofoil S825 for the primary portion, and thin aerofoil S826 for the tip. The 3D geometry of the blade model is illustrated in Figure 1

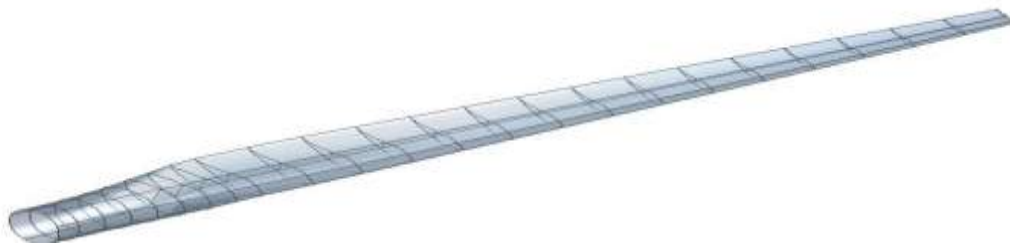


Figure 1 1.5 MW WindPACT wind turbine blade's 3D geometry model

Table 1

Key characteristics of the 1.5 MW Wind PACT wind turbine

Parameters	Value	Unit
Rated power	1.5	MW
No. of blades	3	-
Rotar diameter	86.5	Meter
Rated wind speed	11.5	m/s

Rotational velocity	21.21	Rpm
---------------------	-------	-----

3. FEA modelling

A FEA model of wind turbine composite blades is established using ANSYS Static Structural module which is a widely used FEA modelling software. The FEA model is then applied to the FEA modelling of WindPACT 1.5MW wind turbine blades. ANSYS workbench was used to find the stresses and vibration analysis of the turbine blade. The model of the wind turbine blade was built using SOLIDWORKS, exported to ANSYS/Workbench to start the finite element simulation. The numerical work in this paper covers the steady state and vibration problems of the wind turbine blade. The behaviour of the steady-state of wind turbine blade was investigated due to centrifugal force. It was assumed that the critical case, when the blade works, is at the rated output power (maximum rotational velocity 21.21 RPM). The boundary condition of the wind turbine blade is similar to the cantilever beam, where the blade is fixed at the root and is free at the tip as shown in Figure 2

Table. 2, lists the mechanical properties of the selected materials..In order to obtain the results with a high accuracy, the optimal mesh was selected based on the standard mesh test for both cases static structure analysis and in modal analysis, the selected element size for meshing was 0.1m with quadrilateral element type for two different type of blade used. The number of elements was 19892 Figure 3 illustrates the selected mesh that used for steady-state and vibration analysis.

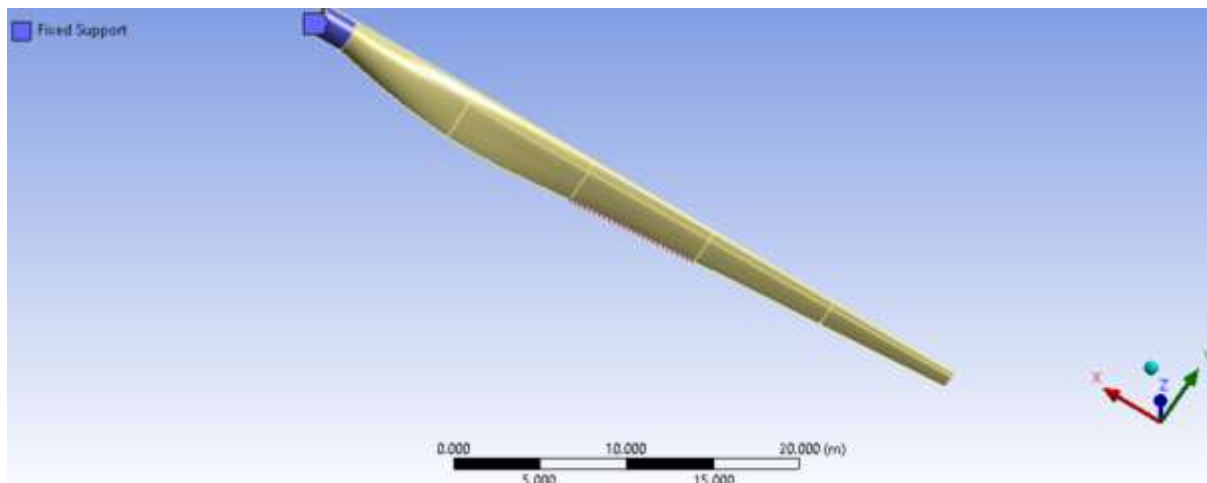


Figure 2 B.C of the wind turbine blade

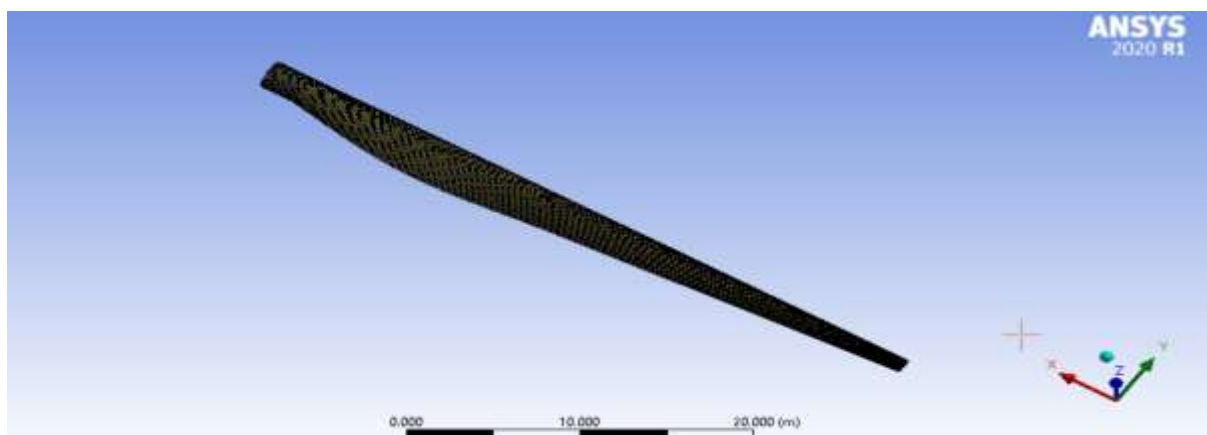


Figure 3 Static structural and model mesh for WindPACT 1.5 MW Blade

Table 2. Mechanical properties of the selected materials of wind turbine blades

Material Name	Elastic modulus (Gpa)	Density (Kg/m3)	Poisson's ratio
E glass	73	2600	.22
S glass	93	2500	.22
Carbon fiber	395	1800	.20

4. RESULTS AND DISCUSSIONS

In this section, the results and vibration analysis are presented. The results display the stresses, deformations and natural frequencies and mode shape of the wind turbine blade. It was assumed during the steady-state domain that the wind turbine works at the maximum allowable rotational velocity (21.1 RPM) to produce the designed rating power. Within this examination, the impact of rotational speed on blade performance was investigated through the utilization of three distinct composite materials: E Glass, S Glass and carbon Fibre. The total deformations, stresses and natural frequencies of the NREL 1500 KW wind turbine blade employing the specified materials are presented. It can be noticed that the distribution of deformation and stress are similar when using three materials (The maximum deformation occurred at the tip region of the blade because it is free to move and the maximum stress occurred in the root region) But the values of stresses and deformation vary with materials. It is evident that stresses and deformations exhibit variation across different materials; the lowest distortion and highest stress values were observed in the case of carbon fiber utilization. The discrepancy arises due to the blade's mass, as an escalation in blade mass results in a corresponding rise in centrifugal force as per the centrifugal force equation ($F=m\omega^2r$).

Tables 3 depict the stress and distortion characteristics of the three materials.

Material	Distortion (m)	Stress (Mpa)
Carbon fibre	.15491	37.1
S Glass	.53863	30.7
E Glass	.6357	29.42

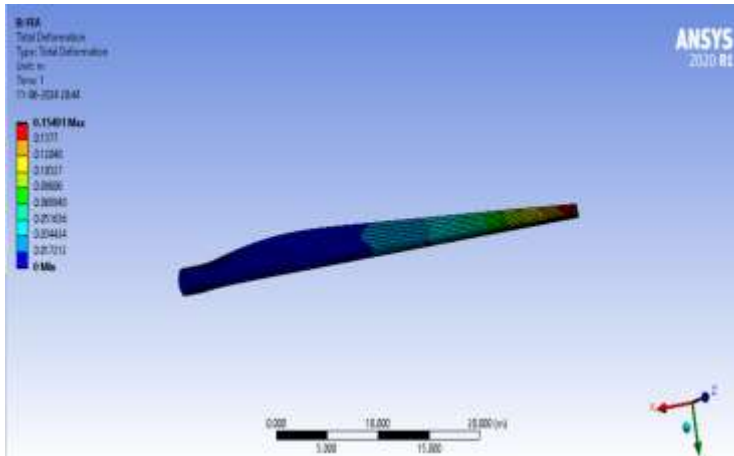


Fig.4 Total distortion of carbon fibre

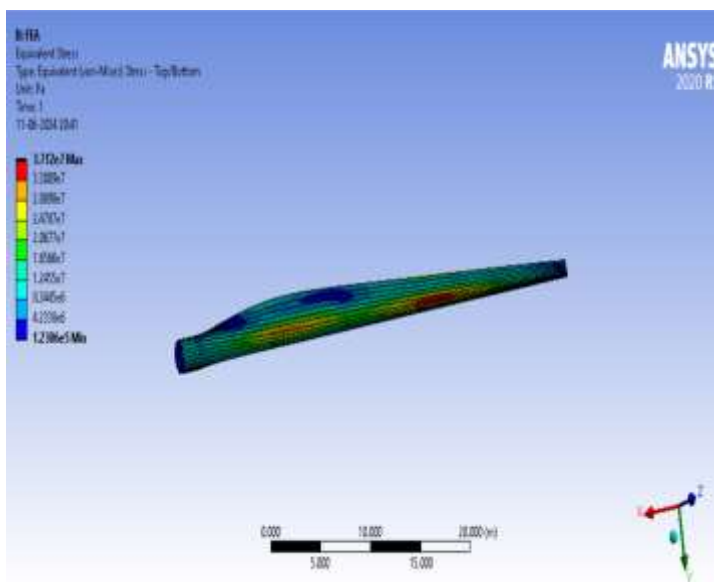


Fig-5 Von-Mises stress distribution of carbon fibre

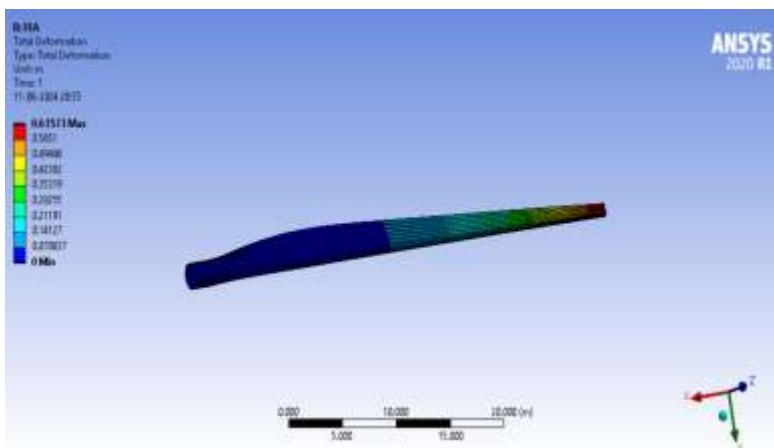


Fig.6 Total distortion of E Glass

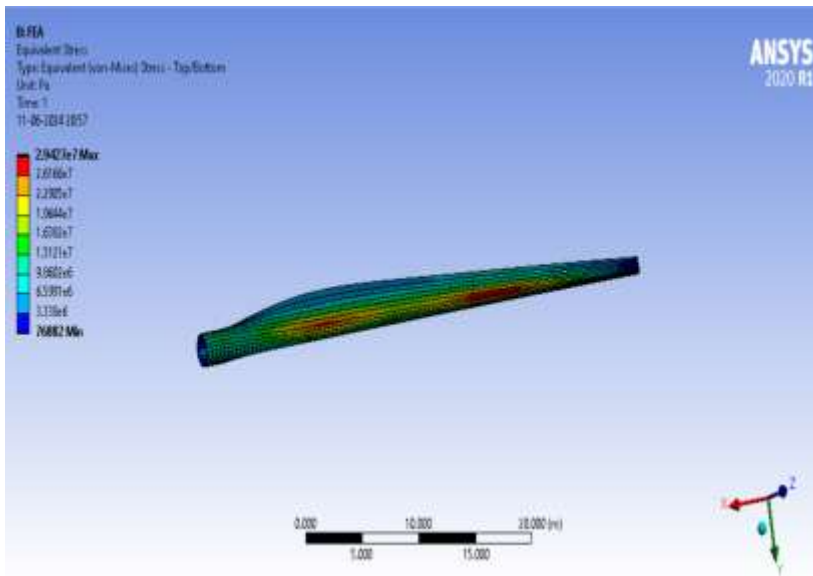


Fig.7 Von-Mises stress distribution of E Glass

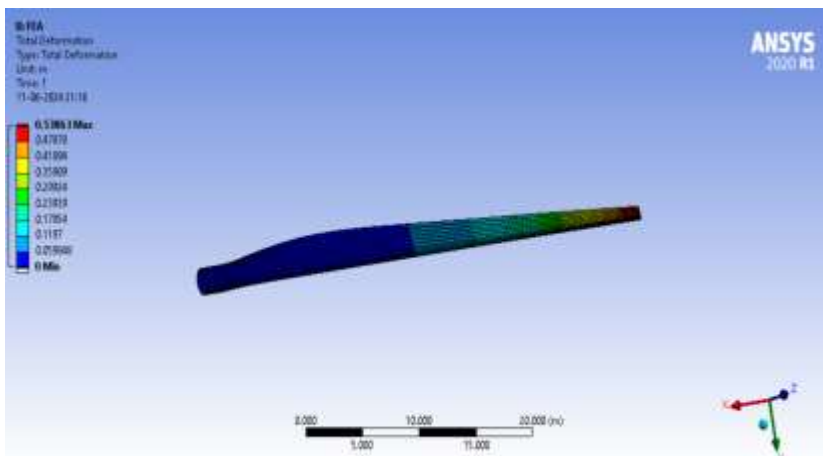


Fig.8 Total distortion of S Glass

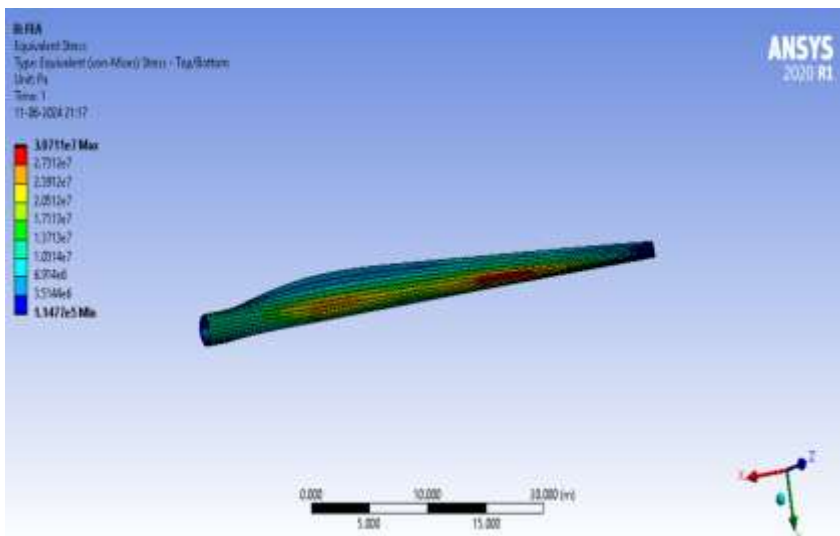


Fig.9 Von-Mises stress distribution of S Glass

Table 4 listed the first eight natural frequencies of the blade when using the selected materials Fig 10-18 exhibit the mode shapes of the blade of wind turbine using the selected materials. It is clear that the values of natural frequency of carbon fibre blade are more than E-glass and S-glass

Table 4 Natural frequency of NREL 1.5 MW blades at different materials

Mode shapes	Natural frequency		
	Carbon fibre	S Glass	E Glass
1	2.7496	1.2747	1.1468
2	5.406	2.868	2.5587
3	7.5699	3.8307	3.392
4	10.894	6.8645	6.094
5	11.924	10.824	9.5657
6	16.157	11.563	10.252
7	17.003	16.875	14.921
8	18.115	19.633	17.375

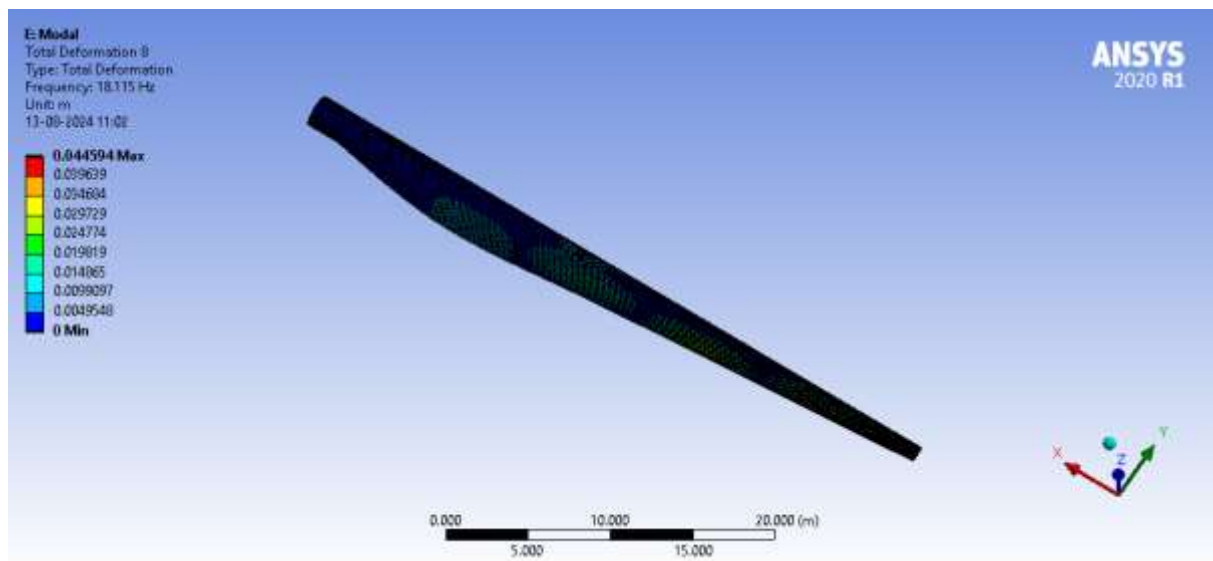


Fig 10 1st mode shape of carbon fiber blade

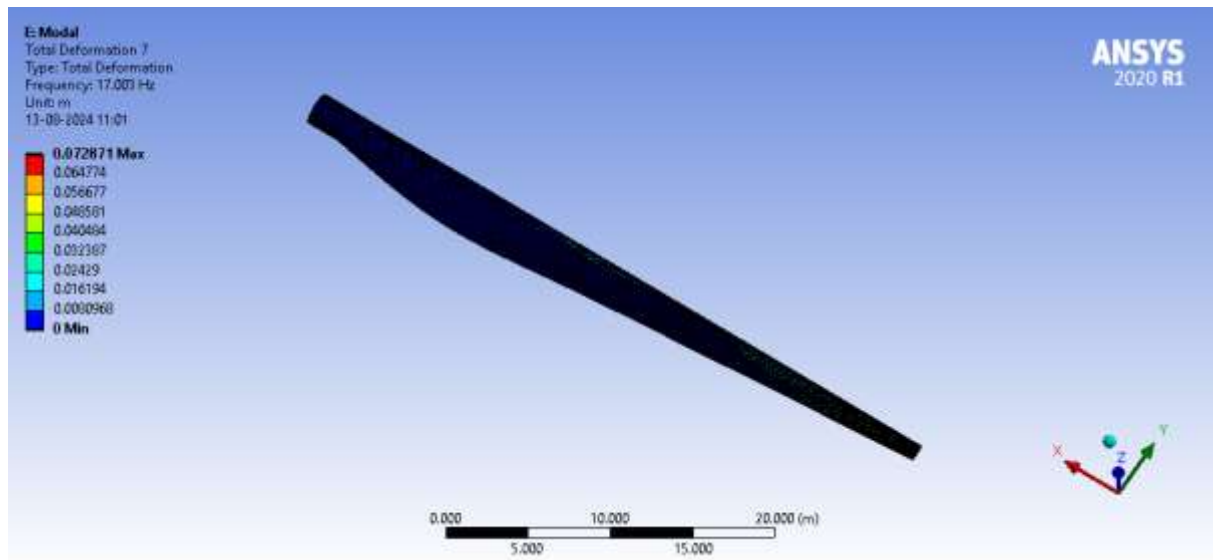


Fig 11 mode shape of carbon fiber blade

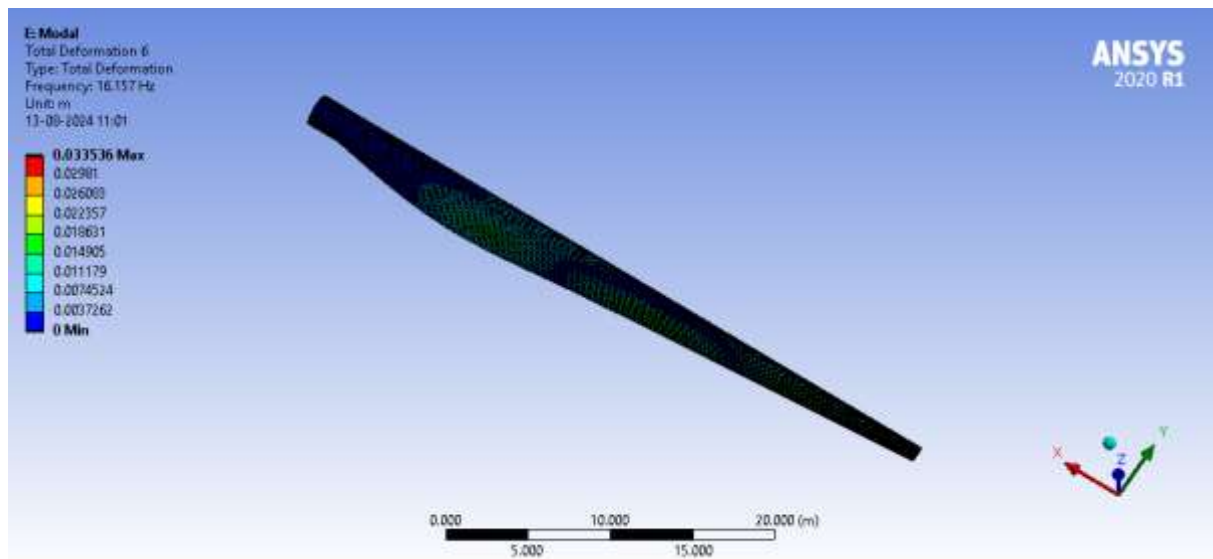


Fig 12 mode shape of carbon fiber blade

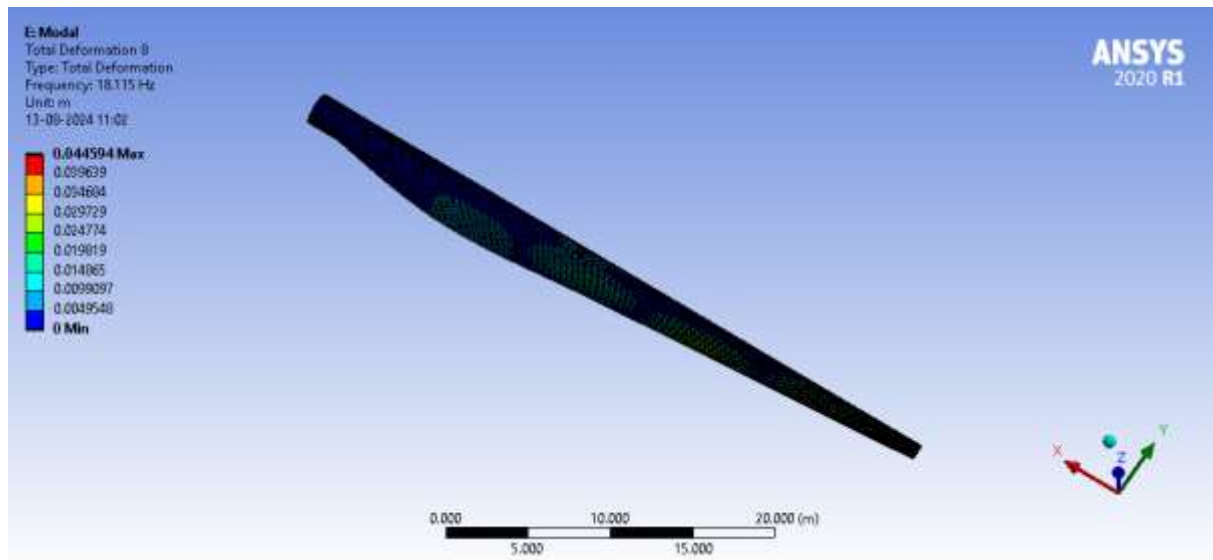


Fig13 1st mode shape of E-Glass blade

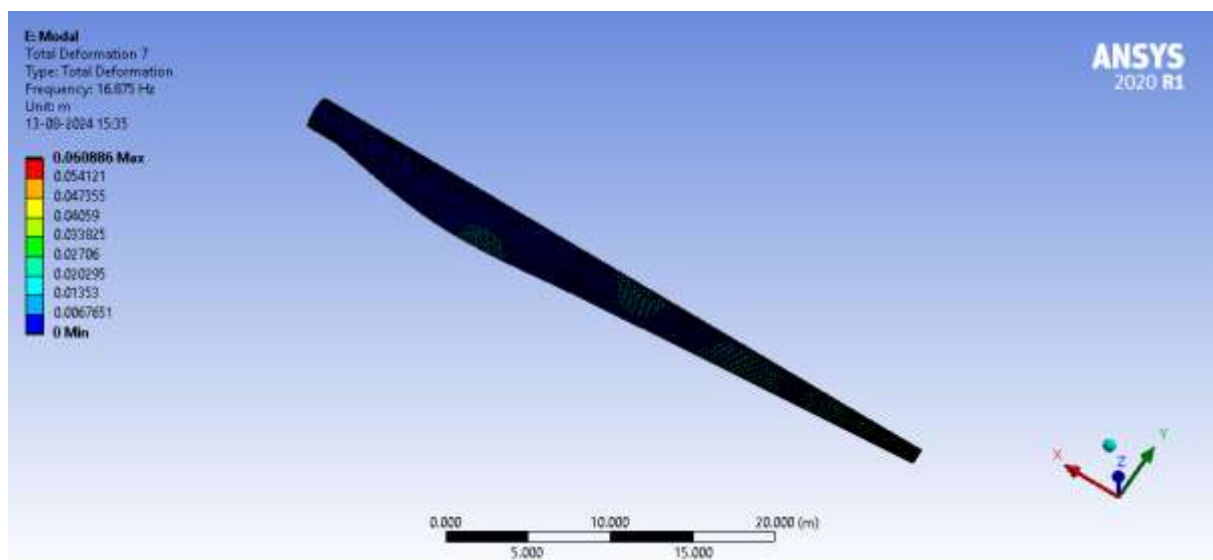


Fig14 2nd mode shape of E-Glass blade

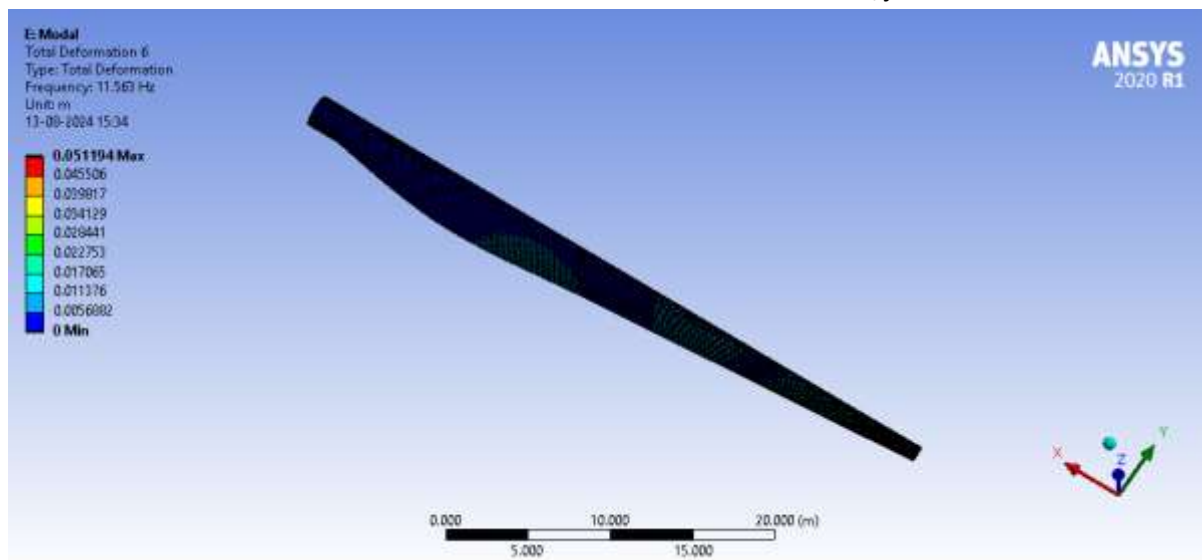


Fig 15 3rd mode shape of E-Glass blade

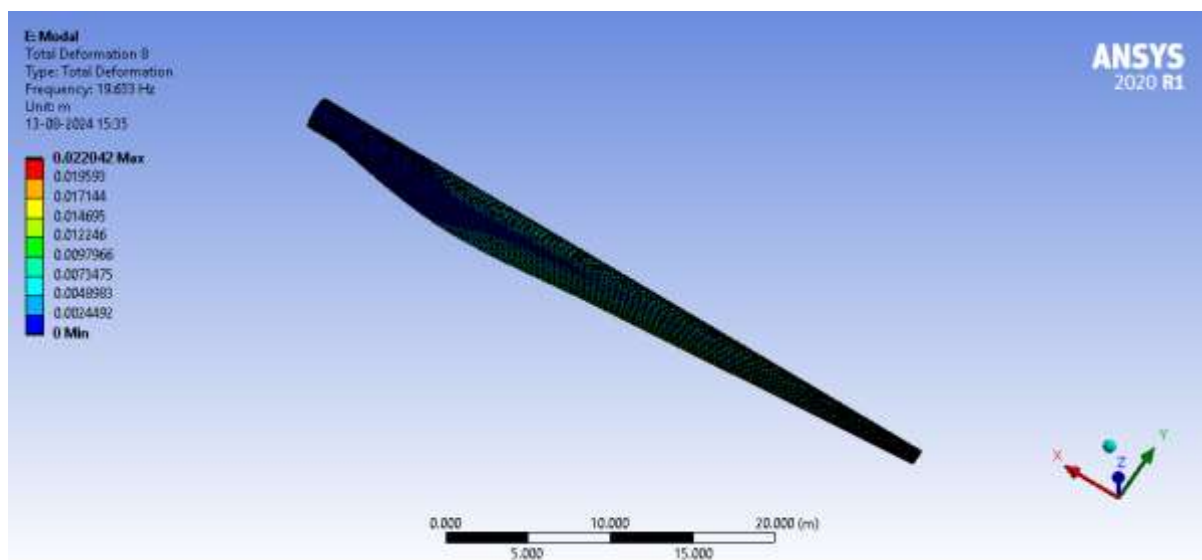


Fig 16 1st mode shape of S-Glass blade

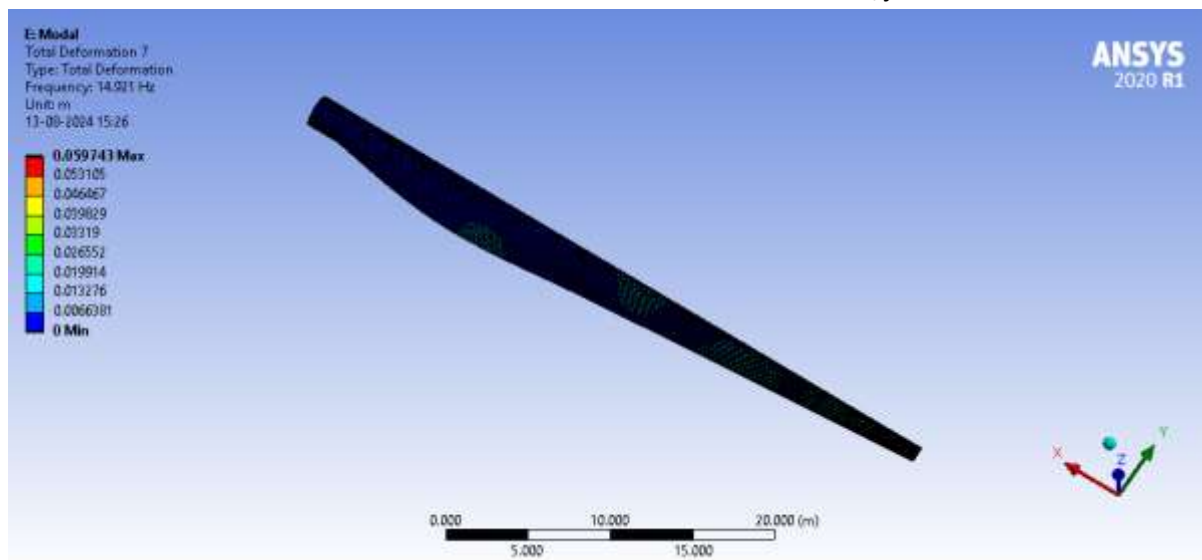


Fig 17 2nd mode shape of S-Glass blade

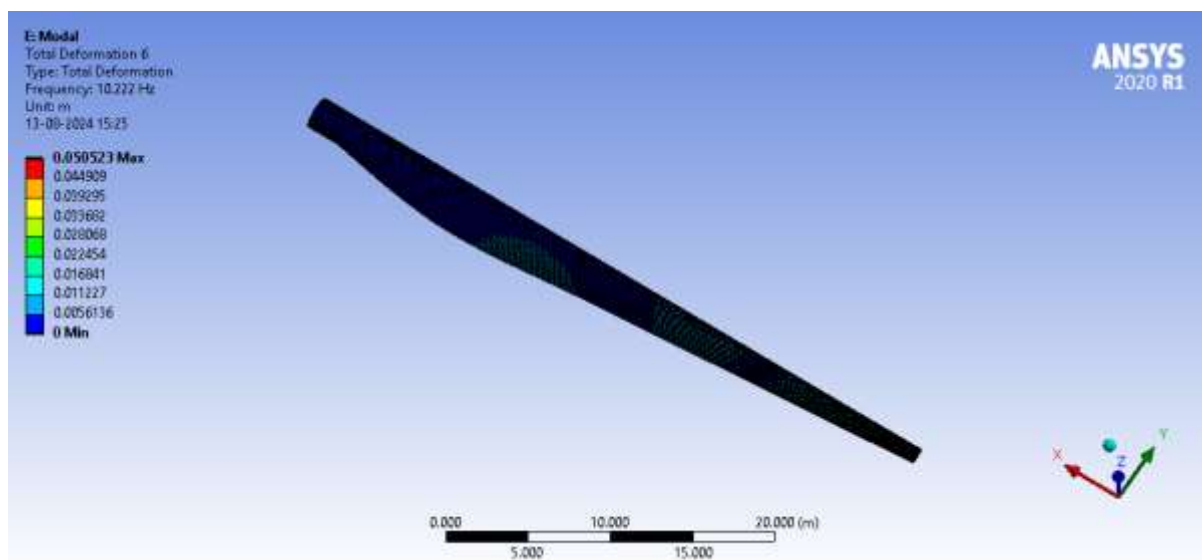


Fig 18 3rd mode shape of S-Glass blade

4.2 Validation of FEA Model

We can determine the aggregate mass and center of mass of the blade within the Ansys software platform. These values serve as essential inputs for the analytical derivation of the root radial force. It is now feasible to compare the computational outcomes of the radial root force with our analytical computations in Table 6

Table 6

Pitch Angle (Degree)	velocity (m/s)	Root radial force (KN)	
		Analytical calculations	CFD analysis
4	12	1465.3 KN	1578.1 KN

5. Conclusion

The finite element method was used to investigate the behaviour of the wind turbine blade under the steady state condition. Furthermore, the vibration characteristics of the selected wind blade were studied deeply. 3-D model of the wind blade was built using SOLID–WORKS software then exported to ANSYS Workbench software to simulate the steady-state and vibration problems

It was determine the stresses ,total deformations and natural frequency and mode shapes of the wind turbine blade. It can be noticed that the distribution of deformation and stress are similar when using three materials (The maximum deformation occurred at the tip region of the blade because it is free to move and the maximum stress occurred in the root region) But the values of stresses and deformation vary with materials. It is evident that stresses and deformations exhibit variation across different materials; the lowest distortion and highest stress values were observed in the case of carbon fiber utilization. The discrepancy arises due to the blade's mass, as an escalation in blade mass results in a corresponding rise in centrifugal force as per the centrifugal force equation ($F=m\omega^2r$)

Reference

- [1] C. Phelps, J. Singleton, "Wind Turbine Blade Design. Cornell University," Sibley School of Engineering, pp. 2-14, 2013.
- [2] Tukesh Singh Thakur, Brijesh Patel, "Structural Analysis of a Composite Wind Turbine Blade to optimize its Constructional Parameters using a FEA Software," IJSRD-International Journal for Scientific Research & Development. Vol. 3. No. 4pp. 572-576, Nov. 2016.
- [3] Armen Sargsyan, "Simulation and modeling of flow field around a horizontal axis wind turbine (HAWT) using RANS method," Florida Atlantic University, 8pp. 7-15, 2010
- [4]. Makridis, A.; Chick, J. Validation of a CFD model of wind turbine wakes with terrain effects. J. Wind Eng. Ind. Aerodyn. 2013, 123, 12–29. [CrossRef]
- [5]. Orlandi, A.; Collu, M.; Zanforlin, S.; Shires, A. 3D URANS analysis of a vertical axis wind turbine in skewed flows. J. Wind Eng. Ind. Aerodyn. 2015, 147, 77–84. [CrossRef]

10.48047/jocaaa.2024.33.07.39

- [6]. Plaza, B.; Bardera, R.; Visiedo, S. Comparison of BEM and CFD results for MEXICO rotor aerodynamics. *J. Wind Eng. Ind. Aerodyn.* 2015, 145, 115–122.
- [7]. Tu, J.; Yeoh, G.H.; Liu, C. *Computational Fluid Dynamics: A Practical Approach*; Butterworth-Heinemann: Oxford, UK, 2018
- [8]. Wang, L.; Liu, X.; Renevier, N.; Stables, M.; Hall, G.M. Nonlinear aeroelastic modelling for wind turbine blades based on blade element momentum theory and geometrically exact beam theory. *Energy* 2014, 76, 487–501. [CrossRef]
- [9]. Sudhamshu, A.R.; Pandey, M.C.; Sunil, N.; Satish, N.S.; Mugundhan, V.; Velamati, R.K. Numerical study of effect of pitch angle on performance characteristics of a HAWT. *Eng. Sci. Technol. Int. J.* 2016, 19, 632–641.
- [10]. Rocha, P.C.; de Araujo, J.C.; Lima, R.P.; da Silva, M.V.; Albiero, D.; de Andrade, C.F.; Carneiro, F.O.M. The effects of blade pitch angle on the performance of small-scale wind turbine in urban environments. *Energy* 2018, 148, 169–178. [CrossRef]
- [11]. Rezaeiha, A.; Kalkman, I.; Blocken, B. Effect of pitch angle on power performance and aerodynamics of a vertical axis wind turbine. *Appl. Energy* 2017, 197, 132–150
- [12]. Ansari, M.; Nobari, M.R.H.; Amani, E. Determination of pitch angles and wind speeds ranges to improve wind turbine performance when using blade tip plates. *Renew. Energy* 2019, 140, 957–969.
- [13]. Colombo, L.; Corradini, M.L.; Ippoliti, G.; Orlando, G. Pitch angle control of a wind turbine operating above the rated wind speed: A sliding mode control approach. *ISA Trans.* 2020, 96, 95–102. [CrossRef] [PubMed]
- [14]. Krueger, B.; Kratz, S.; Theopold, T.; Soter, S. Wear Reduction Control Method in a Blade Pitch System of Wind Turbines. In *Proceedings of the 2019 IEEE 28th International Symposium on Industrial Electronics (ISIE)*, Vancouver, BC, Canada, 12–14 June 2019; pp. 1107–1112.
- [15]. Jiao, X.; Yang, Q.; Fan, B.; Chen, Q.; Sun, Y.; Wang, L. EWSE and Uncertainty and Disturbance Estimator Based Pitch Angle Control for Wind Turbine Systems Operating in Above-Rated Wind Speed Region. *J. Dyn. Syst. Meas. Control* 2020, 3, 142.
- [16]. Yuan, Y.; Chen, X.; Tang, J. Multivariable robust blade pitch control design to reject periodic loads on wind turbines. *Renew. Energy* 2020, 146, 329–341.
- [17]. Civelek, Z. Optimization of fuzzy logic (Takagi-Sugeno) blade pitch angle controller in wind turbines by genetic algorithm. *Eng. Sci. Technol. Int. J.* 2020, 23, 1–9
- [18]. Iqbal, A.; Ying, D.; Saleem, A.; Hayat, M.A.; Mehmood, K. Efficacious pitch angle control of variable-speed wind turbine using fuzzy based predictive controller. *Energy Rep.* 2020, 6, 423–427
- [19] B. Plaza, R. Bardera, and S. Visiedo, "Comparison of BEM and CFD results for MEXICO rotor aerodynamics," *Journal of Wind Engineering & Industrial Aerodynamics*, vol. 145, pp. 115-122, 2015.
- [20] A. Orlandi, M. Collu, S. Zanforlin, and A. Shires, "3D URANS analysis of a vertical axis wind turbine in skewed flows," *Journal of Wind Engineering & Industrial Aerodynamics*, vol. 147, pp. 77-84, 2015.
- [21] A. Makridis and J. Chick, "Validation of a CFD model of wind turbine wakes with terrain effects," *Journal of Wind Engineering & Industrial Aerodynamics*, vol. 123, pp. 12-29, 2013

10.48047/jocaaa.2024.33.07.39

- [22] M. O. L. Hansen, J. N. Sørensen, S. Voutsinas, N. Sørensen, and H. A. Madsen, "State of the art in wind turbine aerodynamics and aeroelasticity," *Progress in aerospace sciences*, vol. 42, pp. 285-330, 2006.
- [23] P. Zhang and S. Huang, "Review of aeroelasticity for wind turbine: Current status, research focus and future perspectives," *Frontiers in Energy*, vol. 5, pp. 419-434, 2011.
- [24] Magdi Ragheb and Adam M. Ragheb. "Wind Turbines Theory-The Betz Equation and Optimal Rotor Tip Speed Ratio," *INTECH open sciences*, 21pp ,2-22, July 5, 2011.
- [25] Wang, L. *Nonlinear Aeroelastic Modelling of Large Wind Turbine Composite Blades*. Ph.D. Thesis, University of Central Lancashire, Preston, UK, 2015.
- [26] Y. Zheng, H. Yang, Coupled fluid structure flutter analysis of a transonic fan, *Chinese J. Aeronautics* 24 (3) (2011) 258–264
- [27] J.-M. Vaassen, P. DeVincenzo, C. Hirsch, B. Leonard, Strong coupling algorithm to solve fluid structure-interaction problems with a staggered approach, in *Proceedings of the 11th International WS on Simulation & EGSE Facilities for Space Programmes*, 2010
- [28] W. Lin, Q. Robin, K. Athanasios, Fluid structure interaction modelling of horizontal-axis wind turbine blades based on CFD and FEA, *J. Wind Eng. Ind. Aerodyn.* 158 (2016) 11–25.
- [29] S. Gilberto, P. Mathijs, V.P. Wim, D. Joris, Fluid–structure interaction simulations of a wind gust impacting on the blades of a large horizontal axis wind turbine, *Energies* 13 (3) (2020) 509.
- [30] M. Panchadarla, K. Syed, Fluid structure interaction analysis of horizontal axis wind turbine, *Int. J. Recent Tech. Eng.* (2020),V.8 I.5.
- [31] H. Glauert, "Airplane propellers," *Aerodynamic theory*, vol. 4, pp. 169-360, 1935
- [32] M. O. L. Hansen, J. N. Sørensen, S. Voutsinas, N. Sørensen, and H. A. Madsen, "State of the art in wind turbine aerodynamics and aeroelasticity," *Progress in aerospace sciences*, vol. 42, pp. 285-330, 2006.
- [33] P. Zhang and S. Huang, "Review of aeroelasticity for wind turbine: Current status, research
- [34] L. Wang, A. Kolios, T. Nishino, P.-L. Delafin, and T. Bird, "Structural optimisation of vertical-axis wind turbine composite blades based on finite element analysis and genetic algorithm," *Composite Structures*, 2016.
- [35] L. Wang, X. Liu, and A. Kolios, "State of the art in the aeroelasticity of wind turbine blades: Aeroelastic modelling," *Renewable and Sustainable Energy Reviews*, vol. 64, pp. 195-210, 2016.
- [36] D. MacPhee and A. Beyene, "Fluid-structure interaction of a morphing symmetrical wind turbine blade subjected to variable load," *International Journal of Energy Research*, vol. 37, pp. 69-79, 2013.
- [37] P. Krawczyk, A. Beyene, and D. MacPhee, "Fluid structure interaction of a morphed wind turbine blade," *International Journal of Energy Research*, vol. 37, pp. 1784-1793, 2013.
- [38] E. Bagheri and A. Nejat, "Numerical aeroelastic analysis of wind turbine NREL Phase VI Rotor," *Energy Equipment and Systems*, vol. 3, pp. 45-55, 2015
- [39] Naji Abdullah Mezaal, K.V. Osintsev and Sergey Alyukov "The computational fluid dynamics performance analysis of horizontal axis wind turbine"